ASTROBIOLOGY
Volume 13, Number 6, 2013
© Mary Ann Liebert, Inc.
DOI: 10.1089/ast.2012.0872

Raman Spectroscopic Analysis of Geological and Biogeological Specimens of Relevance to the ExoMars Mission

Howell G.M. Edwards,[1,2] Ian B. Hutchinson,[2] Richard Ingley,[2] John Parnell,[3] Petr Vítek,[4] and Jan Jehlička[4]

Abstract

A novel miniaturized Raman spectrometer is scheduled to fly as part of the analytical instrumentation package on an ESA remote robotic lander in the ESA/Roscosmos ExoMars mission to search for evidence for extant or extinct life on Mars in 2018. The Raman spectrometer will be part of the first-pass analytical stage of the sampling procedure, following detailed surface examination by the PanCam scanning camera unit on the ExoMars rover vehicle. The requirements of the analytical protocol are stringent and critical; this study represents a laboratory blind interrogation of specimens that form a list of materials that are of relevance to martian exploration and at this stage simulates a test of current laboratory instrumentation to highlight the Raman technique strengths and possible weaknesses that may be encountered in practice on the martian surface and from which future studies could be formulated. In this preliminary exercise, some 10 samples that are considered terrestrial representatives of the mineralogy and possible biogeologically modified structures that may be identified on Mars have been examined with Raman spectroscopy, and conclusions have been drawn about the viability of the unambiguous spectral identification of biomolecular life signatures. It is concluded that the Raman spectroscopic technique does indeed demonstrate the capability to identify biomolecular signatures and the mineralogy in real-world terrestrial samples with a very high degree of success without any preconception being made about their origin and classification. Key Words: Biosignatures—Mars Exploration Rovers—Raman spectroscopy—Search for life (biosignatures)—Planetary instrumentation. Astrobiology 13, 543–549.

1. Introduction

The analytical application of Raman spectroscopy to the identification of the survival strategies of terrestrial extremophiles through the characterization of key molecular biosignatures has provided novel information about the roles of the protective chemicals synthesized by these organisms under the most severe environmentally stressed conditions on Earth, ranging from hot and cold deserts, salterns, hot springs, and glaciers (see for example Wynn-Williams and Edwards, 2000a, 2000b, 2002; Vítek *et al.*, 2010, 2013). Nondestructive sampling requirements and the ability to discriminate between organic biomolecular spectral signatures and those originating from the inorganic or mineral host matrices in the terrestrial geological record are essential for the *in situ* assessment of the survival strategies being employed against low-wavelength, high-energy ultraviolet radiation insolation, extreme desiccation, the presence of toxic chemicals and heavy metals, extremes of high and low temperatures, and nutrient deficiency found in terrestrial extreme habitats that are termed Mars analog sites (Villar and Edwards, 2006). The inclusion of a miniaturized Raman spectrometer (Rull *et al.*, 2011) as a component of the European Space Agency's ExoMars life-detection suite instrument for the molecular and elemental analytical characterization of specimens in the martian surface and subsurface has focused attention on the Raman spectroscopic detection of key biomarkers of life signatures. The proposed search for the biochemical indicators of extinct or extant life signatures on Mars with Raman spectroscopic techniques confirms the importance of assimilating the analytical data relating to extremophilic biocolonization found in terrestrial sites.

The ExoMars mission of the European Space Agency (ESA) and Roscosmos in 2018 is arguably the most ambitious

[1]Centre for Astrobiology and Extremophiles Research, School of Life Sciences, University of Bradford, Bradford, UK.
[2]Department of Physics and Astronomy, Space Research Centre, University of Leicester, Leicester, UK.
[3]Department of Geology and Petroleum Geology, University of Aberdeen, Aberdeen, UK.
[4]Institute of Geochemistry, Mineralogy and Mineral Resources, Faculty of Sciences, Charles University, Prague, Czech Republic.

analytical experiment to search for life signatures on another planet that has ever been envisaged. The ExoMars mission will carry a payload that comprises a combination of molecular and elemental spectroscopic analytical functions whose inclusion on the Pasteur suite of instruments on the Mars rover vehicle is expected to provide information about the martian surface and subsurface geology and biogeology that has not been achievable hitherto. It is clear that a major factor in the drive toward the miniaturization of the Raman spectroscopic instrumentation required for adoption on ExoMars and deployment on the martian planetary surface is the quality of the molecular information that has been forthcoming from Raman spectroscopic studies of extremophilic organisms found in a variety of terrestrial environments where specific survival strategies have been identified. The key to the survival of terrestrial extremophiles in stressed environments at these "limits of life" situations is the synthesis of a suite of biochemical protectants in their adaptation of their geological matrices (Cockell and Knowland, 1999).

Examples of these biochemical protectant molecules are scytonemin, carotenoids, trehalose, porphyrins, and anthraquinone-based pigments; the recognition of these key spectral biomarkers in the Raman spectrum of extinct or extant extremophiles has been demonstrated in the presence of their geological matrices without the necessity of separation techniques or chemical and mechanical treatment being invoked (see for example Ellery and Wynn-Williams, 2003; Edwards *et al.,* 2005a; Vítek *et al.,* 2010). This is particularly advantageous for a remote planetary rover operation such as ExoMars, where the Raman spectrometer is one of the first-pass instruments in the analytical interrogation procedure, where it is critical that the examination of the powdered specimen provided from the surface or subsurface of the martian regolith is undertaken without compromising the ability of successive analytical techniques to operate. Previous laboratory studies of terrestrial extremophiles that colonize a wide range of geological substrates have identified the key biological molecular protectant signatures from which a special group of biologically modified minerals have also been recognized (Cockell and Knowland, 1999; Villar and Edwards, 2006). It is fair to say that in most cases supporting studies have already identified the geological host matrix concerned, and the Raman spectral studies have therefore been concerned more with the interrogation of the geobiological interfaces and identification of the protective biochemicals used in the survival strategies. A detailed consideration of the generic specific biomarker molecules and their Raman spectral identifiers will be the subject of a future paper, but here we have undertaken a "blind test" series of experiments designed to examine the Raman spectral data provided from terrestrial materials that have relevance to the geology of Mars, several of which may contain biological components; it is stressed that these specimens are all naturally occurring terrestrial rocks that have not been pretreated chemically in any way, except for the provision of pulverized samples, which will also apply to the ExoMars mission experiments. As far as we can ascertain, this represents the first time that this approach has been adopted in order to aid the future protocol expected for the ExoMars analytical experiment.

1.1. Raman spectroscopy

Raman spectroscopy is an analytical technique that provides information about the molecular structures and chemical environments of organic and inorganic molecules and molecular ions (Raman and Krishnan, 1928; for comprehensive information regarding the technique see Lewis and Edwards, 2001; Long, 2002). The generation of Raman spectra requires the illumination of target specimens with laser radiation, which can be focused or nonfocused and for which the "footprint" can range from about one micron to several hundred microns in cross-sectional diameter depending upon the optical design of the sample illuminator. Raman spectra are observed as two sets of wavelength-shifted bands from the Rayleigh line, which occurs at the frequency of the incident laser radiation; the long-wavelength set of Raman bands comprise the Stokes Raman spectrum, and the low-wavelength set comprise that of the anti-Stokes Raman spectrum, which is relatively weaker in intensity compared with the Stokes Raman spectrum (Edwards, 2000; Edwards and Carter, 2001).

The position of Raman bands is commonly expressed in wavenumbers (cm^{-1}) and designated as Raman shift. Because the Raman effect has an inverse dependence upon the fourth power of the laser wavelength, much Raman spectroscopy has been carried out in the visible region of the electromagnetic spectrum with the use of blue and green wavelengths. However, the advent of nonvisible wavelength diode lasers operating in the ultraviolet and the near-infrared regions has provided some novel sources of excitation of Raman spectra; currently, there are reports of Raman spectra being excited at wavelengths of 240 nm in the deep ultraviolet and at 1330 nm in the near-infrared region, and with all other instrumental factors being equal, power for power, the Raman spectrum excited in the ultraviolet will be some 950× more intense than that recorded in the near-infrared region over this wavelength range.

A major disadvantage of Raman spectroscopy excited in the blue-green spectral region is the onset of an intense fluorescence emission that arises from the laser probing of the electronic levels of the specimen (Long, 2002). Fluorescence emission is several orders of magnitude greater in intensity than the corresponding Raman scattering generated by the same laser wavelength, and relatively intense, broadband fluorescence backgrounds can generally swamp the much weaker Raman bands from the same sample. From detailed work studies undertaken by the space agencies, the selection of the optimum instrumental requirements and experimental conditions for the generation of Raman spectra has been formulated, and the excitation wavelength of choice is 532 nm, which is situated in the green region of the electromagnetic spectrum. In the present study, we have used laboratory Raman spectrometers (with diode and argon ion laser excitation at different wavelengths) to interrogate a range of specimens (described below) on a blind test basis.

1.2. Molecular specificity

The presence or otherwise of Raman spectral signatures is indicative of the composition of a specimen, but some materials are inherently weaker than others in Raman scattering based on the concept of molecular scattering coefficients; this means that Raman spectra will consist of strong and weak

features, but the weaker bands are not necessarily those arising from the minor components in a mixture. The sensitivity of Raman spectroscopy for the observation of Raman bands depends upon the polarizability change in electronic charge density of the chemical bonds within a molecular system on excitation with laser irradiation (Edwards, 2000; Edwards and Carter, 2001; Long, 2002). Generally, bonds between large, polarizable atoms give rise to strong Raman spectra where the number of Raman bands observed is dictated by the molecular symmetry through the operation of spectroscopic selection rules; the more symmetric a molecule, the fewer the Raman bands that are obtained in the spectrum. The positions of the Raman bands are also dictated by the type of molecular bond that is being irradiated; Raman bands originating from bonds between heavy atoms will occur in a low Raman shift region of the spectrum. For example, mercury (II) sulfide has a very strong and characteristic Raman band at 253 cm^{-1}, whereas a carbon-hydrogen bond in an aliphatic hydrocarbon will occur near 2950 cm^{-1}. This gives rise to the molecular specificity of Raman spectra, whereby it is possible to recognize the presence of molecules or chemical moieties from the positions of their Raman bands. This is the basis of diagnostic analysis, in which the observation of key features in the Raman spectra of molecules is indicative of a molecular presence. Hence, the presence of a band in the Raman spectrum of keratotic proteins at about 500 cm^{-1} is a diagnostic verification of S-S bonding; furthermore, the change in the Raman shift of this feature occurs in a verifiable way (Lewis and Edwards, 2001; Edwards *et al.*, 2005a), with conformation about the C-S-S-C linkage in the protein. Localized cis, trans, and gauche conformational structures can be identified diagnostically between 480 and 520 cm^{-1}.

In these Raman spectra, the effect of the coordinated water in different sites in the crystal matrix upon the vibrational modes of the oxalate molecular ions is apparent in the area of Raman shift of the stretching and bending bands of the $C_2O_4^{2-}$ ions. The CO bond stretching Raman shift occurs at 1493, 1468 cm^{-1} for whewellite and 1476 cm^{-1} for weddellite, with corresponding C-O bending modes at 506 and 494 cm^{-1}, respectively. The recognition of these two materials in the geological record is significant for life-detection experiments since these materials are found to remain even after the life processes that produced them have ceased to exist (Bouchard and Smith, 2003). It should be noted that Raman spectroscopy depends upon the interactions of electromagnetic radiation with chemical bonds for the production of a spectrum. Hence, a Raman spectrum would not be expected from monatomic ions, such as Ca^{2+}, Na^{+}, and Mg^{2+}. However, as has been noted in the case of the molecular electronic environments in the vicinity of water molecules evident in the differences observed for the weddellite and whewellite spectra, the electronic environmental effects of monatomic cations upon molecular anions can also be observed diagnostically in the Raman spectrum even when these cations themselves have no Raman spectrum. This is generally the basis of mineral diagnostic differentiation in Raman spectroscopy, for example, between calcite and aragonite, two polymorphs of $CaCO_3$. Here, the Raman C-O symmetric stretching band of the CO_3^{2-} ion, which is common to these two minerals, occurs at 1086 cm^{-1}. It is interesting that, although calcite and aragonite have an identical stretching Raman band at 1086 cm^{-1}, which effectively means that this is not diagnostically useful for discriminating between these two polymorphs and can merely serve to identify calcium carbonate in a mineral matrix, the two polymorphs can be distinguished from the different Raman shifts exhibited by the other bands in their spectra, namely, 712/704 and 283/206 cm^{-1}, respectively, for calcite/aragonite. A similar situation exists for the two magnesium minerals dolomite, $CaMg(CO_3)_2$, and magnesite, $MgCO_3$, where the CO_3^{2-} stretching band occurs at 1094 cm^{-1} for both minerals, and it is now essential to use the other Raman-active bands for differentiation purposes, for example, 713/738 cm^{-1} and 300, 177, 156/330, 120 cm^{-1}, respectively, for dolomite/magnesite. This highlights a very important point in diagnostic spectroscopy, namely, that it is often not practicable to rely on just one defining band for characterization purposes and that sometimes up to three features need to be considered (Bouchard and Smith, 2003).

2. Methods

2.1. Specimens

All specimens were provided as numbered, powdered samples with no information about their source geology and the presence or otherwise of biological colonization (extinct or extant). Sample information:

(1) Gypsum/iron oxide crust from soil zone, Haughton Crater, Devon Island, Canadian Arctic (potential significance: evaporitic areas, iron oxide dust documented on Mars)
(2) Microbial carbonate crust, Haughton Crater (potential significance: evaporitic areas documented on Mars, missions looking for microbial colonization on Mars)
(3) Cyanobacteria-coated pebbles, Haughton Crater (potential significance: missions looking for microbial colonization on Mars)
(4) Carbonaceous matter-rich shale, Port Selma, Scotland, UK (potential significance: missions looking for microbial colonization on Mars, possibility of detection of carbonaceous matter as residue of extinct organisms)
(5) Red mudstone with annelid borings, Larne, Northern Ireland, UK (potential significance: liquid water role in sediment formation, iron oxide particles documented on Mars)
(6) Red stromatolite, Precambrian, Clachtoll, Scotland, UK (potential significance: missions looking for microbial colonization on Mars, possibility of detection of carbonaceous matter as residue of extinct organisms, stromatolites represents primitive biogenic assemblages on Earth)
(7) Basalt with weathered exterior crust, Helen's Bay, Northern Ireland, UK (potential significance: basaltic zones documented on Mars, limits of biomarker/carbon detection by Raman spectroscopy)
(8) Organic-rich black shale, Orkney, Scotland, UK (potential significance: limits of biomarker/carbon detection by Raman spectroscopy)
(9) Weathered red basalt, Giant's Causeway, Northern Ireland, UK (potential significance: basaltic zones documented on Mars, limits of biomarker/carbon detection by Raman spectroscopy)

(10) Sandstone with lichenous weathered surface, Vale of Eden, England, UK (potential significance: basaltic zones documented on Mars, limits of biomarker/pigment detection by Raman spectroscopy)

Because of the heterogeneity of the powdered specimens, spectral stackplots of the raw data are presented with separate spectra for each of the identified sample phases (mineral grains, aggregates identified with a microscope). The Raman shift range in each plot is 100–2000 cm^{-1}, which contains the expected functional group signatures of most common minerals and organic compounds of biological relevance.

2.2. Spectrometer details

The 10 powdered samples were analyzed with two separate spectrometers: a Horiba Scientific LabRAM HR Raman microscope equipped with a 532 nm excitation laser (laser power in the range 0.2–10 mW) and an InVia Raman microscope with options for both 785 and 514.5 nm excitation (principally 785 nm excitation was used as a universal source for interrogation of both inorganic and organic phases, although the significant fluorescence exhibited by samples 7, 8, and 10 demonstrated the benefit of illumination at a wavelength of 514.5 nm). The laser spot diameter on the LabRam spectrometer was varied between 7 and 100 μm (depending on which of the 10×, 50×, or 100× microscope objectives was used) and was fixed at 4 μm for the InVia system (using a 50× objective). Data acquisition times varied between 10 and 30 s depending on the Raman efficiency and background fluorescence of each individual sample, with multiple accumulations (up to 20) needed in some cases. Several regions on the surface of each powder were investigated in order to sample the different phases present in each sample.

3. Results

Sample 1 (Fig. 1) shows the presence of gypsum (top spectrum), goethite, and pyrite within a gypsum matrix. There is no evidence in the spectrum for any organic species in this sample. Sample 2 (Fig. 2) shows an aragonite matrix, minor calcite, and dolomite, with bands due to scytonemin. In Sample 3 (Fig. 3), a dolomite matrix is seen to contain green aggregates, and Sample 4 (Fig. 4) has a mixed inorganic matrix of quartz, pyrite, feldspar, and hematite, with clear signals of disordered carbon (A, B, C) showing the D and G at around 1312 and 1579 cm^{-1}, respectively. Sample 5 (Fig. 5) shows an inorganic composition of calcite and minor anatase, quartz, and hematite with broad spectral bands between 1200 and 1700 cm^{-1}. Sample 6 (Fig. 6) is basically

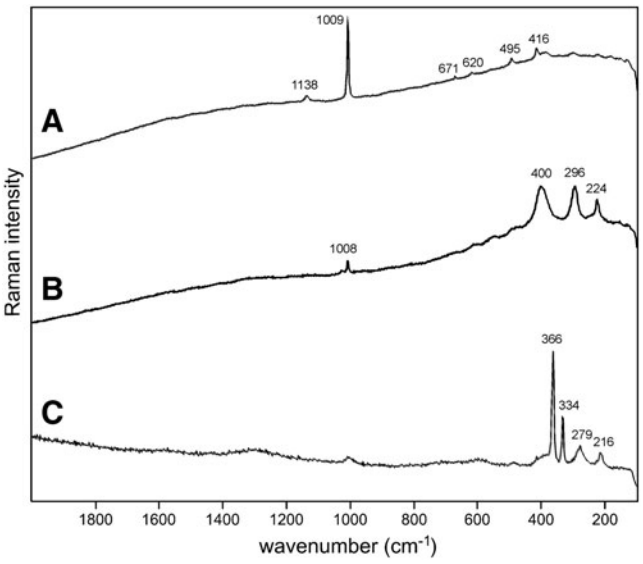

FIG. 1. Sample 1 (785 nm excitation). (**A**) Gypsum matrix, (**B**) goethite, (**C**) pyrite with minor hematite.

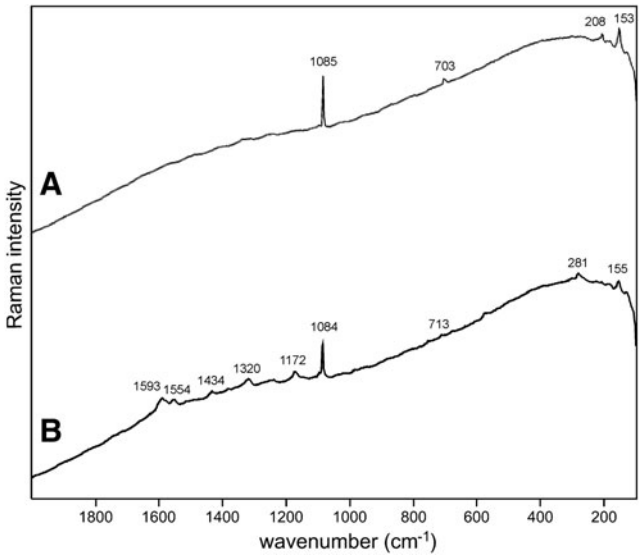

FIG. 2. Sample 2 (785 nm excitation). (**A**) Aragonite matrix; (**B**) aragonite with clear features of UV-protective pigment scytonemin between 1150 and 1600 cm^{-1} corroborated by weak bands below 800 cm^{-1}.

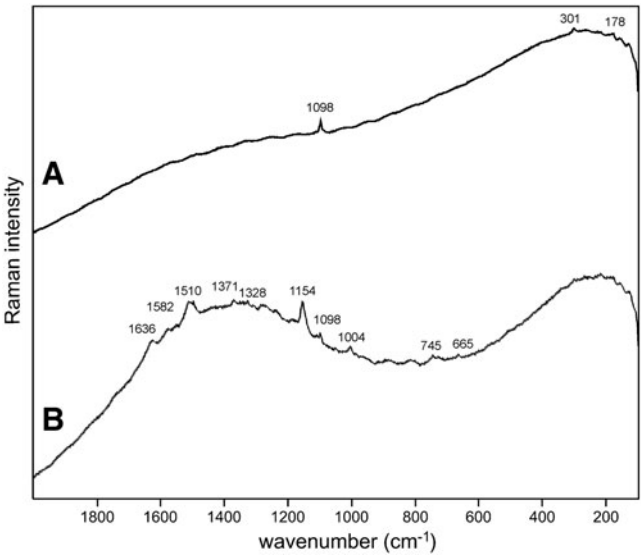

FIG. 3. Sample 3 (785 nm excitation). (**A**) Dolomite signal with relative high fluorescence background; (**B**) bands of three different pigments are evident on fluorescence background between 600 and 1650 cm^{-1}—carotenoid, chlorophyll, and phycobiliproteins, which are typical for cyanobacteria.

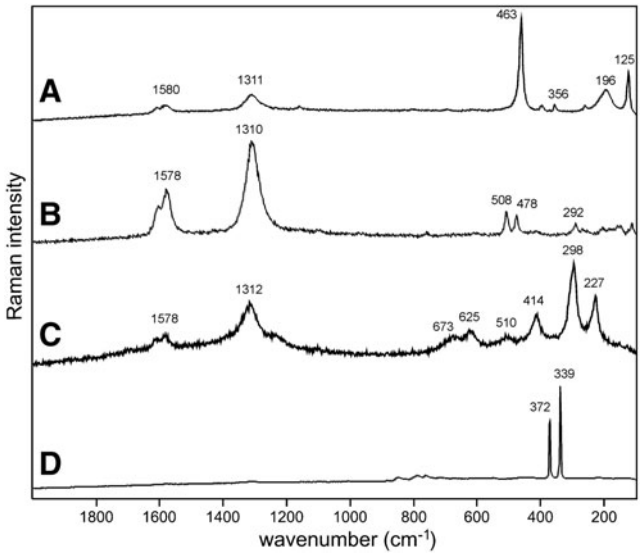

FIG. 4. Sample 4 (785 nm excitation). (**A**) Clear signatures of disordered carbon (1300–1600 cm^{-1}) and quartz (below 500 cm^{-1}); (**B**) strong disordered carbon signal with two peaks of feldspar and very weak features of hematite (below 600 cm^{-1}); (**C**) disordered carbon and clear hematite features below 700 cm^{-1}, note the shoulder at around 1320 cm^{-1} representative of disordered hematite; (**D**) pyrite.

composed of quartz and hematite but also includes broad signals between 1200 and 1700 cm^{-1}. Sample 7 (Fig. 7) has strong signals for anatase and hematite, and G and D carbonaceous matter bands (spectra 7A and 7B), with the three bands characteristic of a carotenoid (spectrum 7C). Sample 8 (Fig. 8) has a matrix of calcite and dolomite, with a characteristic doublet at 1095 and 1086 cm^{-1} as seen in spectrum A and carbon. In Sample 9 (Fig. 9), the essential compounds

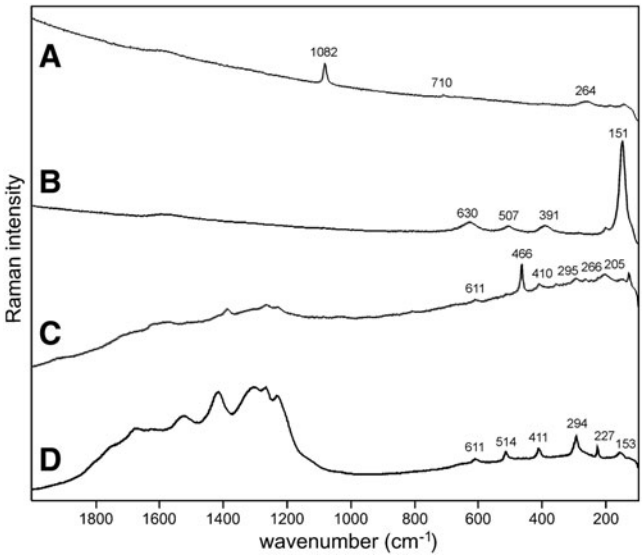

FIG. 5. Sample 5 (785 nm excitation). (**A**) Calcite; (**B**) anatase; (**C**) quartz with broad features between 1200 and 1800 cm^{-1} tentatively suggested as signs of the presence of the highly condensed network of polycyclic aromatic hydrocarbons; (**D**) hematite (below 700 cm^{-1}) with broad features similar to those in the spectrum above.

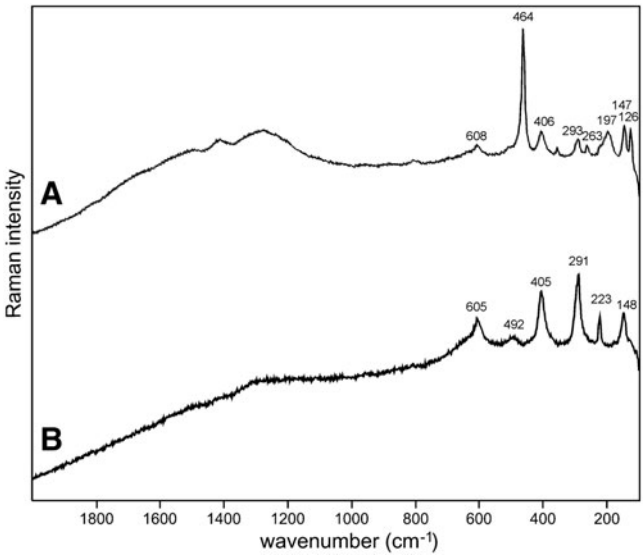

FIG. 6. Sample 6 (785 nm excitation). (**A**) Quartz with minor disordered hematite described on some parts of the Apex Chert samples (Marshall *et al.*, 2011); (**B**) hematite.

identified were hematite and anatase with isolated localized aggregate rich in carotenoids (spectrum C). Sample 10 (Fig. 10) was recognized as predominantly a quartz matrix with several green spots from which clear carotenoid signal (spectrum B) was recorded by using both 785 and 514.5 nm excitation sources, with weak chlorophyll signal observed by the 785 nm laser as well.

4. Discussion

There is no evidence for any organic species in the spectra obtained from Sample 1, but bands associated with

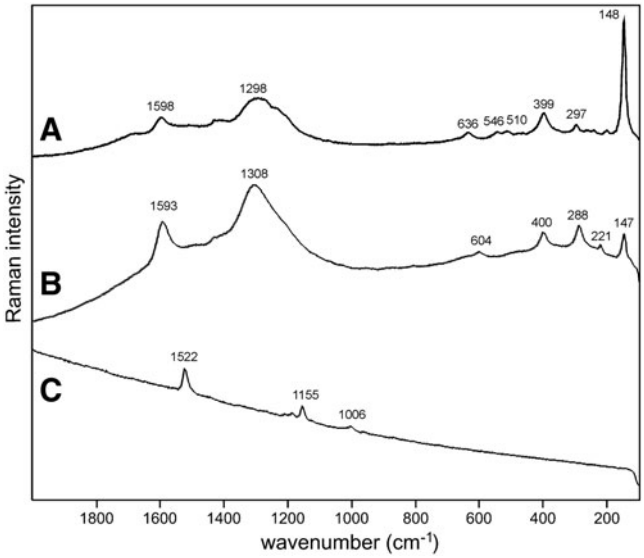

FIG. 7. Sample 7 (514.5 nm excitation). (**A**) anatase; (A) and (B) G and D carbonaceous matter bands between 1100 and 1600 cm^{-1}; (**B**) hematite; (**C**) clear carotenoid signal between 1000 and 1550 cm^{-1}.

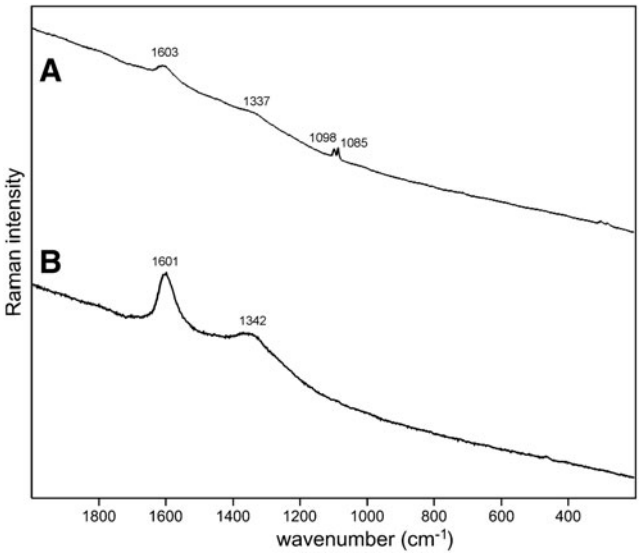

FIG. 8. Sample 8 (514.5 nm excitation). The sample was fluorescent at 785 nm, and slope of fluorescence is present also when 514.5 nm excitation was used, but with observable Raman features. (**A**) Matrix with calcite and dolomite peaks 1086 and 1098 cm^{-1}, respectively (calcite is prevailing through the sample); very broad features of disordered carbon are present as well between 1300 and 1650 cm^{-1}. (**B**) Broad Raman features of disordered carbon.

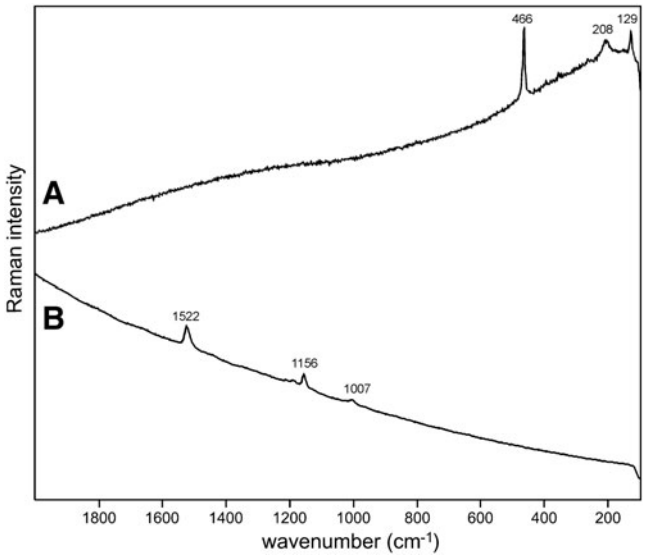

FIG. 10. Sample 10 (514.5 nm excitation). (**A**) quartz matrix, (**B**) clear carotenoid signal from green aggregates.

scytonemin are clearly seen in Sample 2. Scytonemin is a low-wavelength UVB and UVC absorber that is a biomarker of cyanobacterial colonization (Edwards *et al.*, 2005b; Villar *et al.*, 2006). Analysis of the green aggregates seen in Sample 3 indicates that they are carotenoids, chlorophyll, and phycobilins, and there are also clear signals of cyanobacterial colonization.

Both of the carbon bands seen in Sample 4 spectra are relatively narrow, but Fig. 4C indicates additionally the presence of a shoulder at around 1320 cm^{-1} documenting together with other Raman features in the lower area of the spectrum, in this case, the presence of hematite together with disordered carbonaceous matter. This shoulder can easily be confused with the carbon-related A1g Raman band, and care must be taken when interpreting spectra in this area, as suggested by Marshall *et al.* (2011).

The broad spectral features between 1200 and 1700 cm^{-1} seen in Sample 5 may be due to the presence of a highly condensed network of polycyclic aromatic hydrocarbons. The very broad signals between 1200 and 1700 cm^{-1} in the spectra from Sample 6 can be compared to disordered hematite described on some parts of the Apex Chert samples (Marshall *et al.*, 2011).

An interesting feature seen in the spectra obtained from Sample 8 is the broad character and intensity ratio of the D and G bands reflecting the low ordering of the disordered carbon in this sample in contrast with the spectrum shown for Sample 4. The general shape of the spectrum (broad bands, sloping baseline) indicates lower thermal maturity when compared to the carbonaceous matter of Sample 4. The spectrum of disordered carbon in Sample 4 has a pronounced high Raman shift shoulder on the G-band arising possibly from higher pressure alteration of the carbonaceous matter, which is absent from the corresponding spectrum in Sample 8.

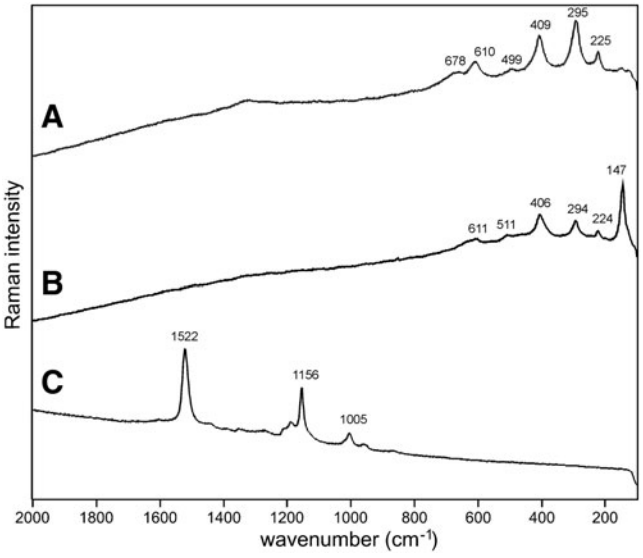

FIG. 9. Sample 9 (785 nm excitation). (**A**) Hematite, (**B**) anatase with hematite, (**C**) clear carotenoid signal from green aggregate.

4.1. Conclusions

The Raman spectroscopic analyses of these powdered specimens of 10 terrestrial rocks that potentially contain biological and biogeological signatures proved to be an effective description of the samples. The biological signatures are not compromised by their geological counterparts and indicate evidence for the biological colonization where this occurs; in several cases, the presence of carbonaceous matter signals could indicate that thermal degradation of biomolecules has occurred in the geological matrix. Contrary to some initial expectation, the loss of spatial analytical

information arising from a pulverizing of the rock specimens does not actually seem to have an overly adverse effect on the ability of the instrumental technique adopted to determine the presence or otherwise of organic signatures in mineral matrices. What is also clear is that it is fundamentally necessary to undertake multipoint sampling in the pulverized samples here to determine the overall analytical description of the rock specimen; a single point "snapshot" spectrum of any powdered sample is not sufficient to produce a reliably accurate analytical result. For this reason, the proposed decision to undertake multipoint sequential Raman spectra from each pulverized sample on the ExoMars mission seems to be the correct protocol, though the larger laser spot-size of the miniaturized spectrometer on board the ExoMars rover compared to the instrumentation used here may be further advantageous in this context.

What is not yet clear from these experiments is the operational limit of detection that applies for this experimental arrangement and performance of miniaturized Raman instrumentation with larger laser spot-size in this regard; future experiments will be directed toward this objective by using synthetic samples with known concentrations of biomarkers in pulverized mineral matrices.

Acknowledgments

H.G.M.E., I.H., and R.I. acknowledge the support of the STFC Research Council in the UK ExoMars programme. J.J. and P.V. acknowledge the support of the Grant Agency of the Czech Republic (210/10/0467) and of the Ministry of Education of the Czech Republic (MSM0021620855).

References

Bouchard, M. and Smith, D.C. (2003) Catalogue of 45 reference Raman spectra of minerals concerning research in art history or archaeology, especially on corroded metals and coloured glass. *Spectrochim Acta A Mol Biomol Spectrosc* 59:2247–2266.

Cockell, C.S. and Knowland, J.S. (1999) Ultraviolet radiation screening compounds. *Biol Rev Camb Philos Soc* 74:311–345.

Edwards, H.G.M. (2000) Spectra–structure correlations in Raman spectroscopy. In *Handbook of Vibrational Spectroscopy,* Vol. 3, edited by J.M. Chalmers and P.R. Griffiths, John Wiley & Sons, Chichester, pp 1838–1918.

Edwards, H.G.M. and Carter, E.A. (2001) Biological applications of Raman spectroscopy. In *Infrared and Raman Spectroscopy of Biological Molecules,* Practical Spectroscopy Series, Vol. 24, edited by H.U. Gremlich and B. Yan, M. Dekker, New York, pp 421–476.

Edwards, H.G.M., Moody, C.D., Villar, S.E.J., and Wynn-Williams, D.D. (2005a) Raman spectroscopic detection of key biomarkers of cyanobacteria and lichen symbiosis in extreme Antarctic habitats: evaluation for Mars lander missions. *Icarus* 174:560–571.

Edwards, H.G.M., Villar, S.E.J., Parnell, J., Cockell, C.S., and Lee, P. (2005b) Raman spectroscopic analysis of cyanobacterial gypsum halotrophs and relevance for sulfate deposits on Mars. *Analyst* 130:917–923.

Ellery, A. and Wynn-Williams, D.D. (2003) Why Raman spectroscopy on Mars? A case of the right tool for the right job. *Astrobiology* 3:565–579.

Lewis, I.R. and Edwards, H.G.M., Eds. (2001) *Handbook of Raman Spectroscopy: From Research Laboratory to the Process Line,* M. Dekker, New York.

Long, D.A. (2002) *The Raman Effect: A Unified Treatment of the Theory of Raman Scattering by Molecules,* John Wiley & Sons, Chichester.

Marshall, C.P., Emry, J.R., and Marshall, A.O. (2011) Haematite pseudomicrofossils present in the 3.5 billion-year-old Apex Chert. *Nat Geosci* 4:240–243.

Raman, C.V. and Krishnan, K.S. (1928) A new type of secondary radiation. *Nature* 121:501–502.

Rull, F., Maurice, S., Diaz, E., Tato, C., Pacros, A., and the RLS Team. (2011) The Raman Laser Spectrometer (RLS) on the ExoMars 2018 rover mission [abstract 2400]. In *Proceedings of the 42nd Lunar and Planetary Science Conference: Instrumentation and Payload Concepts,* Lunar and Planetary Institute, Houston.

Villar, S.E.J. and Edwards, H.G.M. (2006) Raman spectroscopy in astrobiology. *Anal Bioanal Chem* 384:100–113.

Villar, S.E.J., Edwards, H.G.M., and Benning, L.G. (2006) Raman spectroscopic and scanning electron microscopic analysis of a novel biological colonisation of volcanic rocks. *Icarus* 184: 158–169.

Vítek, P., Edwards, H.G.M., Jehlička, J., Ascaso, C., de los Ríos, A., Valea, S., Villar, S.E.J., Davila, A.F., and Wierzchos, J. (2010) Microbial colonization of halite from the hyper-arid Atacama Desert studied by Raman spectroscopy. *Philos Trans A Math Phys Eng Sci* 368:3205–3221.

Vítek, P., Cámara-Gallego, B., Edwards, H.G.M., Jehlička, J., Ascaso, C., and Wierzchos, J. Phototrophic community in gypsum crust from the Atacama Desert studied by Raman spectroscopy and microscopic imaging. *Geomicrobiol J* 30:399–410.

Wynn-Williams, D.D. and Edwards, H.G.M. (2000a) Proximal analysis of regolith habitats and protective biomolecules *in situ* by laser Raman spectroscopy: overview of terrestrial Antarctic habitats and Mars analogs. *Icarus* 144:486–503.

Wynn-Williams, D.D. and Edwards, H.G.M. (2000b) Antarctic ecosystems as models for extraterrestrial surface habitats. *Planet Space Sci* 48:1065–1075.

Wynn-Williams, D.D. and Edwards, H.G.M. (2002) Environmental UV radiation: biological strategies for protection and avoidance. In *Astrobiology: The Quest for the Origins of Life,* edited by G. Horneck and C. Baumstarck-Khan, Springer, Berlin, pp 245–260.

Address correspondence to:
Ian B. Hutchinson
Department of Physics and Astronomy
Space Research Centre
University of Leicester
University Road
Leicester LE1 7RH
UK

E-mail: ibh1@star.le.ac.uk

Submitted 14 May 2012
Accepted 13 April 2013